VA-89-6-4

Natural Convection and Air Flow Pattern in a Partitioned Room with Turbulent Flow

F. Haghighat, Ph.D.
Associate Member ASHRAE

Z. Jiang

J.C.Y. Wang, Ph.D.
Member ASHRAE

ABSTRACT

Recent studies have emphasized the importance of the interzone air movement in a building and demonstrated the need for better understanding of this movement in any attempt to predict the ventilation efficiency or thermal performance of the building.

This paper discusses the use of the k-ε two-equation turbulence model to simulate natural convection of high Rayleigh number in a partitioned enclosure for a few cases. The airflow in all cases is considered to be three-dimensional owing to the asymmetry of the room configuration. The predictions of the model are compared to available experimental and theoretical results; good agreement is obtained. The study also discusses the effect of door height and location on the pattern of airflow and temperature. Results indicate that the flow pattern is quite sensitive to the variations of door height and location, while the convective heat transfer rate is only sensitive to variation of door height.

INTRODUCTION

While the mechanism of radiation and conduction in the temperature range applicable to buildings is well defined, convective heat transfer processes are usually dealt with in an imprecise way. Recent research results have emphasized the importance of the convection process in the thermal behavior of a building and shown the need for accurate knowledge of this process in predicting the building thermal performance and air quality control. Gadgil et al. (1982) showed that the building heating load calculated by standard building energy analysis methods may have substantial errors as a result of their use of common assumptions regarding the convection processes that occur in an enclosure.

Air movement in a building is caused by a temperature difference between the warm and cold zones (natural convection), by mechanical systems (forced convection), or by a combination of both. The air movement plays a fundamental role in the distribution of heat within the occupied room and between rooms in a multi-zone building, in the thermal comfort (along with thermal radiation), and in the control of air quality. This movement is influenced by the dimensions of the room, air infiltration, the number of outdoor walls, size of the windows, the amount of insulation, and the outside weather conditions. The air movement along with heat and mass transfer can be described by a set of conservation equations: the continuity, momentum, energy, and component conservation equations. For the case of turbulent flows, one or two extra conservation equations are involved. Since no exact solution to these coupled nonlinear differential equations is available, measurement and numerical techniques have been used to investigate the heat and mass transfer and the flow pattern in enclosures.

Investigations on the interzonal heat and mass transfer have been carried out mainly by experimental measurements (Brown and Solvason 1962; Shaw 1972; Wray and Weber 1979; Weber and Kearney 1980; Mahajan 1986, 1987). In experimental studies, correlationships between the Nusselt number, Nu, and the Rayleigh number, Ra, were obtained using the measured temperatures and measured heat flux. The experimental correlations given in Brown and Solvason (1962), Scott et al. (1988), and Nansteel and Greif (1984) show the effects of variable aperture size on the convective heat transfer. In Scott et al. (1988) and Neymark et al. (1988), two different types of flows in a partitioned room driven by a bulk density regime or a boundary layer regime were investigated and the transition between the two types of flow was determined. Generally speaking, experimental investigations may not provide enough information about the flow patterns that are directly related to the heat and mass transfer and the contaminant distribution. This is due to the fact that the air movement in a complex enclosure is affected by many parameters, such as the dimensions of the room, the size and location of the partition opening, and the conditions of the walls, ceiling, and floor. It is difficult to deal with the variations of each of these parameters in an experimental study. A few numerical studies on natural convection in single enclosures were conducted (Markatos and Pericleous 1984; Kubleck et al. 1980; Neilson et al. 1979; Jones and O'Sullivan 1985; Gadgil 1979). Chang et al. (1982) numerically studied laminar natural convection in a two-dimensional partitioned enclosure for the Rayleigh number, Ra, up to 10^8. However, when the Rayleigh number increases to more than 10^9, the transition from laminar flow to turbulent flow may take place (Cheesewright 1968). The mechanism of a turbulent transportation is completely different from the laminar one. For a partitioned enclosure, an opening in the partition will introduce a disturbance to the passing airflow, which enhances the flow turbulence. Furthermore, the two-dimensional flow approximation cannot be accepted in the case of two zones connected through a doorway, since the velocities

The authors are with the Centre for Building Studies, Concordia University, Montreal, Quebec, Canada.

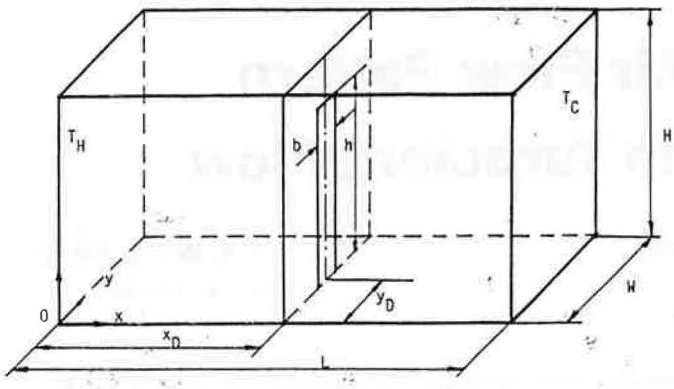

Figure 1 *Configuration of partitioned room*

in the third direction (Figure 1, in y direction) should not be neglected. Consequently, there is a necessity to develop a three-dimensional computational model for predicting the inter- and intrazonal convective heat transfer under turbulent conditions and to have a better understanding of the air movement in a partitioned room and the impact of the door height and location on the air movement. The purpose of the present paper is to investigate numerically the effects of the door size and location on the flow pattern and the interzonal heat transfer rate caused by natural convection in a partitioned enclosure under turbulent flow conditions.

Problem Statement

The physical problem concerns a three-dimensional rectangular enclosure of L·W·H = 10·4·3 m^3 with a partition having an opening (Figure 1). The two opposite end-walls parallel to the partition are at different constant temperatures, T_H and T_c, respectively, while the ceiling, the floor, the partition, and the other walls are assumed to be well insulated. The temperature difference between the warm and cold walls causes a natural convection heat flow through the opening. This convective heat transfer is modeled for variable temperature differences between the hot and cold walls, for variable door dimensions (represented by h/H), and for different door locations (represented by x_D/L and y_D/W, respectively), as shown in Figure 1. In the present study the door width, b/W = 0.25, is kept constant.

Mathematical Model

The natural convective heat transfer process of the aforementioned problem is governed by the following conservation equations:

$$\frac{\partial}{\partial t}(\rho\phi) + \frac{\partial}{\partial x}(\rho u\phi) + \frac{\partial}{\partial y}(\rho v\phi) + \frac{\partial}{\partial z}(\rho w\phi) = \frac{\partial}{\partial x}(\Gamma_\phi \frac{\partial \phi}{\partial x}) + \frac{\partial}{\partial y}(\Gamma_\phi \frac{\partial \phi}{\partial y}) + \frac{\partial}{\partial z}(\Gamma_\phi \frac{\partial \phi}{\partial z}) + S_\phi \quad (1)$$

where ϕ represents each of the three velocity components u, v, and w, the enthalpy, h, the kinetic energy of turbulence, k, and the dissipation rate of the kinetic energy of turbulence, ϵ. The value of ϕ is equal to 1 for the continuity equation. γ_ϕ is the effective exchange coefficient for the property ϕ. S_ϕ is the source term, which is given in detail in Table 1. The k-ϵ two-equation model of turbulence is employed in this study. The local turbulent transportation coefficient is determined in the following form:

TABLE 1
Source Terms for Conservation Equations

ϕ	Γ_ϕ	S_ϕ
1	0	0
u	μ_{eff}	$-\frac{\partial p}{\partial x} + \frac{\partial}{\partial x}(\mu_{eff}\frac{\partial u}{\partial x}) + \frac{\partial}{\partial y}(\mu_{eff}\frac{\partial v}{\partial x}) + \frac{\partial}{\partial z}(\mu_{eff}\frac{\partial w}{\partial x})$
v	μ_{eff}	$-\frac{\partial p}{\partial y} + \frac{\partial}{\partial x}(\mu_{eff}\frac{\partial u}{\partial y}) + \frac{\partial}{\partial y}(\mu_{eff}\frac{\partial v}{\partial y}) + \frac{\partial}{\partial z}(\mu_{eff}\frac{\partial w}{\partial y})$
w	μ_{eff}	$-\frac{\partial p}{\partial z} + \frac{\partial}{\partial x}(\mu_{eff}\frac{\partial u}{\partial z}) + \frac{\partial}{\partial y}(\mu_{eff}\frac{\partial v}{\partial z}) + \frac{\partial}{\partial z}(\mu_{eff}\frac{\partial w}{\partial z})$
h	$\frac{\mu_{eff}}{\sigma_t}$	0
k	$\frac{\mu_{eff}}{\sigma_k}$	$G_k - \rho\epsilon + G_B$
ϵ	$\frac{\mu_{eff}}{\sigma_\epsilon}$	$C_1\frac{\epsilon}{k}(G_k + G_B)(1 + C_3R_f) - C_2\frac{\rho\epsilon^2}{k}$

$$G_k = \mu_{eff}\left[2\left[\left(\frac{\partial u}{\partial x}\right)^2 + \left(\frac{\partial v}{\partial y}\right)^2 + \left(\frac{\partial w}{\partial y}\right)^2\right] + \left(\frac{\partial u}{\partial y} + \frac{\partial v}{\partial x}\right)^2 + \left(\frac{\partial u}{\partial z} + \frac{\partial w}{\partial x}\right)^2 + \left(\frac{\partial v}{\partial z} + \frac{\partial w}{\partial y}\right)^2\right]$$

$$\mu_t = C_d\, C_\mu\, \rho\, k^2/\epsilon \quad (2)$$

where C_d and C_μ are experimentally determined constants. In Table 1, the source term, S_ϕ, of the conservation equation of k consists of three terms in which G_k is the stress production term and G_B is a generation term related to the buoyancy:

$$G_B = -\beta g \frac{\mu_t}{\sigma_t}\frac{\partial (T-T_0)}{\partial z} \quad (3)$$

where T_o is a reference temperature. This equation indicates the exchange between the kinetic energy of turbulence and the potential energy of the flow. In a stable stratification flow G_B becomes a sink term so that the turbulent mixing is reduced while the potential energy is increased. The constants appearing in the k-ϵ two-equation model shown in Table 1 are assigned the following values, which were recommended by Launder and Spalding (1974).

$C_1 = 1.44$ $C_2 = 1.92$ $C_\mu = 0.09$ $C_d = 1.0$
$\sigma_k = 1.0$ $\sigma_\epsilon = 1.3$

The coefficient C_3 (see Table 1), which is the multiplier of the flux Richardson number (R_f), is an additional buoyancy constant. Its value should be close to zero for the vertical buoyancy shear layer and close to unity for horizontal layers (Rodi 1984).

CALCULATION PROCEDURE AND BOUNDARY CONDITIONS

The room considered is divided into 16·10·10 control volumes (cells). The differential conservation equations are integrated over each of the control volumes to obtain the discretization equations of finite difference form

$$a_p\phi_p = a_E\phi_E + a_W\phi_W + a_N\phi_N + a_S\phi_S + a_T\phi_T + a_B\phi_B + b\,, \quad (4)$$

where a_i are the neighbor coefficients representing the convection and diffusion flux at the cell boundary surfaces.

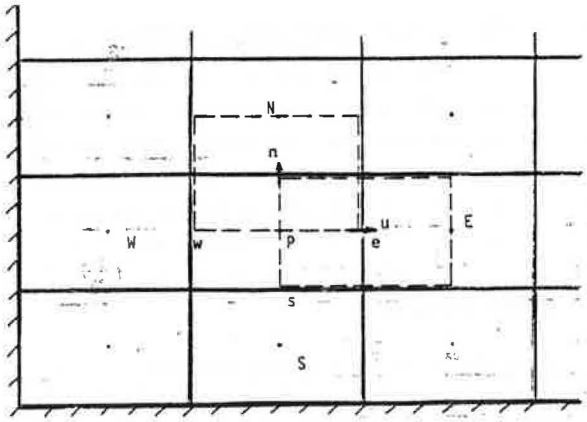

Figure 2 *Control volume and grids*

The subscripts E, W, N, S, T, and B represent the neighbor grids of grid P, as shown in Figure 2. The hybrid scheme, which gives realistic behavior for the both high- and low-cell Peclet numbers, is used to determine the expression of the neighbor coefficients (Patankar 1980). The neighbor coefficients are in the following forms:

$$a_E = [0.5F_e, D_e] - 0.5F_e$$
$$a_W = [0.5F_w, D_w] + 0.5F_w$$
$$a_N = [0.5F_n, D_n] - 0.5F_n$$
$$a_S = [0.5F_s, D_s] + 0.5F_s$$
$$a_T = [0.5F_t, D_t] - 0.5F_t$$
$$a_B = [0.5F_b, D_b] + 0.5F_b$$
$$b = S_c \Delta x\Delta y\Delta z + a_P^\circ \phi_P^\circ$$
$$a_P^\circ = \rho_P^\circ \Delta x\Delta y\Delta z/\Delta t$$
$$a_P = a_E + a_W + a_N + a_S + a_T + a_B + a_P^\circ - S_P\Delta x\Delta y\Delta z \qquad (5)$$

where e, w, n, s, t, and b represent the boundary of the control volume. The symbol [ ] stands for the largest of the quantities contained within it. S_c and S_p are from linearization of the source term S_ϕ (Patankar 1980). a_P°, ϕ_P°, and ρ_P° refer to the values at the previous time step. The boundaries of the control volume for the determination of the scalar variables T, k, and ϵ are identical to the physical boundaries. For the velocity components u, v, and w, the staggered control volumes are employed; that is, the grid points for the velocity components u, v, and w are located at the centers of the boundary surface of the control volume for the scalar variables (Figure 2). The SIMPLE algorithm (Patankar 1980) used for the solution of the finite difference equations is modified by adding an overall-continuity correction in x-direction to ensure the mass balance at the aperture where the flow properties are changed rapidly. The false time step and the ADI (Alternative Direction Im-

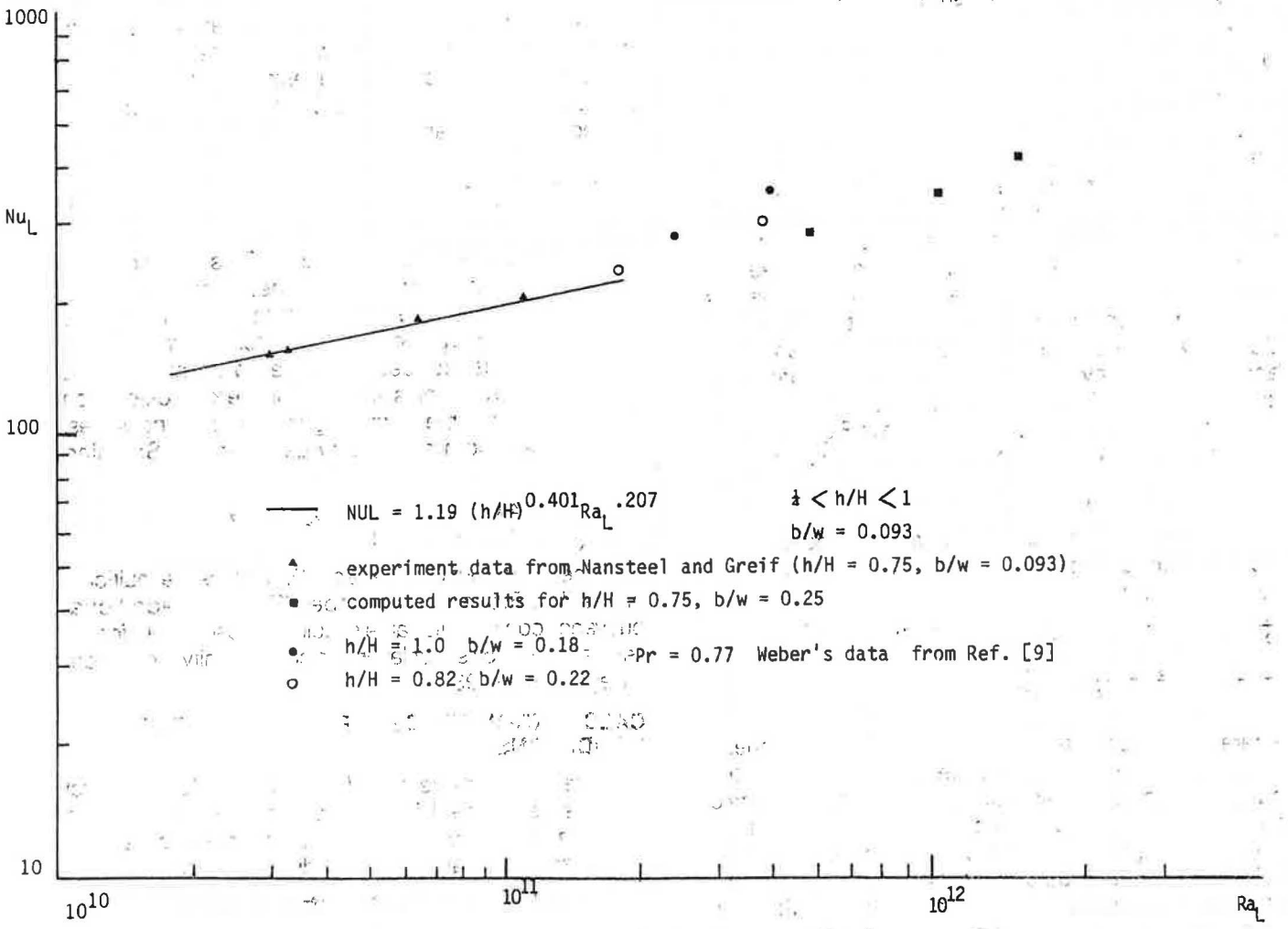

Figure 3 *Comparison with experimental measurements*

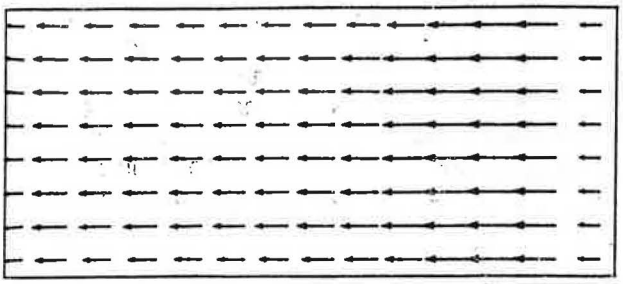

a) x-y plane at y/H = 0.06215

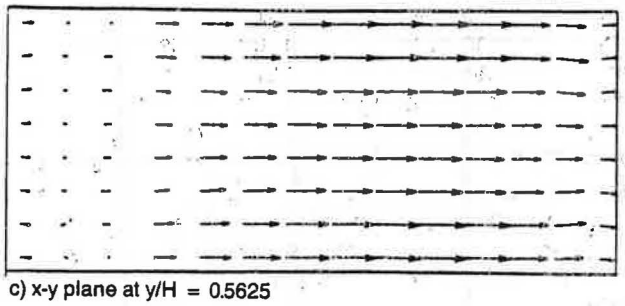

c) x-y plane at y/H = 0.5625

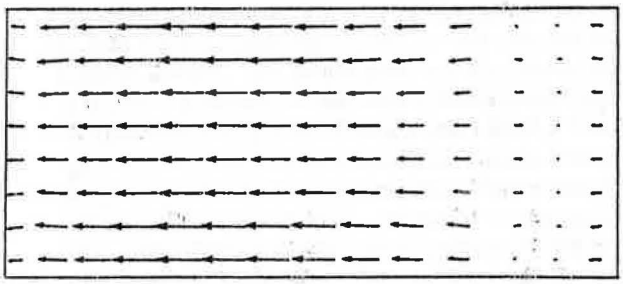

b) x-y plane at y/H = 0.4375

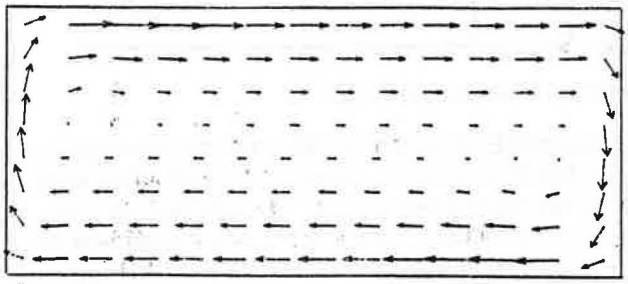

d) x-z plane at y/W = 0.5625

Figure 4 *Velocity vectors in x-y and x-z planes for the case without partition*

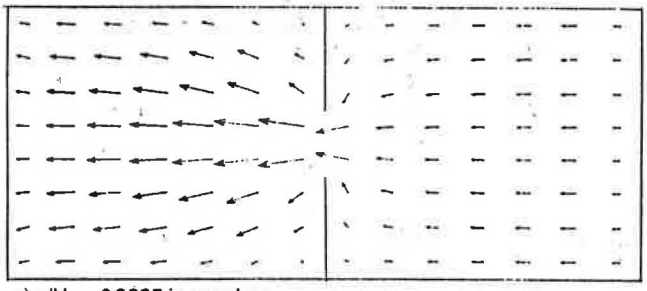

a) z/H = 0.0625 in x-y plane

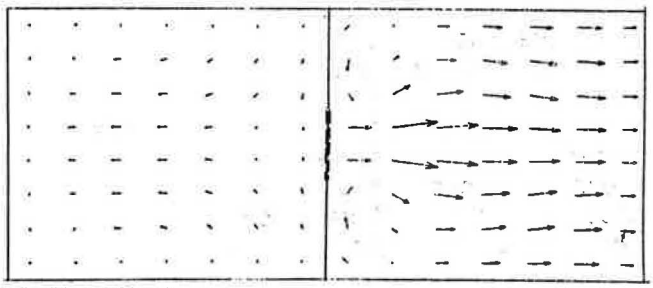

d) z/H = 0.8125 in x-y plane

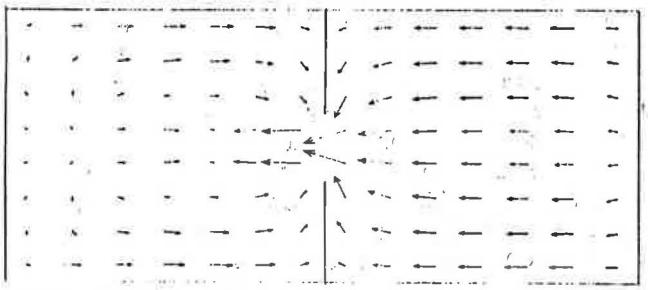

b) z/H = 0.3125 in x-y plane

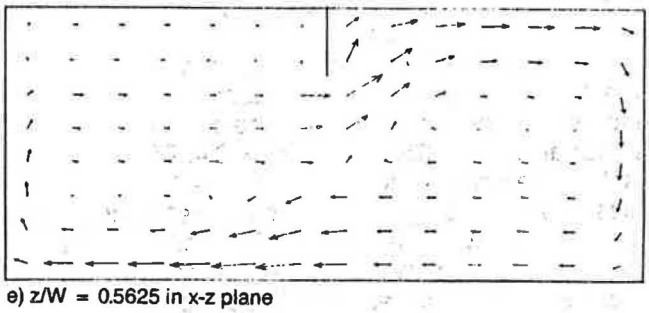

e) z/W = 0.5625 in x-z plane

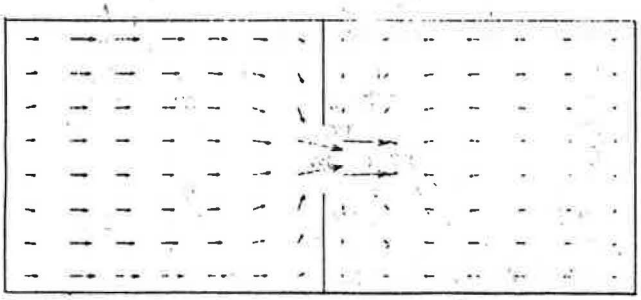

c) z/H = 0.5625 in x-y plane

Figure 5 *Velocity vectors in x-y and x-z planes for the case with the door (h/H = 0.75) at the middle of the partition*

plicit) iterative procedure are adopted in our computations. The non-slip condition at the solid surfaces is applied for velocities. Insulated conditions at the partition, the insulated walls, floor, and ceiling are used for the energy equation. Zero of turbulence kinetic energy and zero gradient of dissipation rate of turbulence kinetic energy are considered for k and ϵ at solid surfaces. Turbulent wall functions (Launder and Spalding 1972) are applied to describe flow properties at the grids near the solid walls. The Nusselt number is calculated from the average convective heat flux at the hot and cold walls.

RESULTS

The comparison of the computed Nusselt number, Nu_L, as a function of the Rayleigh number, Ra_L, with experimental results reported in Nansteel and Greif (1984) is shown in Figure 3. The boundary conditions in our computation are chosen so that they are the same as those used in Nansteel and Greif (1984). Since the cell size is restricted by the number of grids, the parameter b/W, which is 0.25 in the calculation, does not exactly match the value adopted in Nansteel and Greif (1984). The computed values of Nu_L lie on a higher Ra_L region than those values obtained in Nansteel and Greif (1984). From Figure 3 it can be seen that the numerical results calculated from the computational model are in good agreement with the experimental data. The convective heat transfer rates cited in Nansteel and Greif (1984) are also plotted in Figure 3.

Figure 4 displays the velocity vectors for the case without partition. In the x-z plane (Figure 4d), a typical natural convection loop, as shown in the experiment of Chen (1988), is observed. There is a core region in the center of the enclosure where the velocities are relatively small. A weak vortex is shown at the hot side above the mid-height of the enclosure. Another vortex appears in the cold side below the mid-height. This phenomenon was also reported in Markatos and Pericleous (1984) for the case of Ra over 10^6. The velocity vectors in x-y plane reveal that in a single enclosure the velocity in y direction is negligible (Figures 4 a,b,c). A two-dimensional approximation for numerical simulation is acceptable. In the planes parallel to the floor at z/H = 0.0625 and z/H = 0.4375, the air moves from the cold wall toward the hot wall while the velocities at z/H = 0.5625 are in the opposite direction, from the hot wall toward the cold wall. The neutral plane (velocities in x-direction are equal to zero) is at about mid-height of the room for the case without partition.

Figure 5 illustrates the flow patterns in the room divided by a partition with a centrally located door of h/H = 0.75 and b/W = 0.25. When a partition is inserted in the room, the two-dimensional feature no longer exists, especially for the case of the door located closer to a side-wall (Figures 10b,c). In Figure 5 it is observed that the airflow near the floor at z/H = 0.0625 moves from cold zone into the hot zone. At the height z/H = 0.3125 the air in the hot zone starts to change its flow direction from the hot wall toward the cold wall, while the air in the cold zone still moves toward the hot wall. The horizontal counterflows interact in the hot zone. A similar phenomenon occurs in the cold zone at the height z/H = 0.5625. Figure 5e shows that the neutral levels in the hot and cold zones are not at the same height. In the hot zone, the neutral level (for the cross section of y/W = 0.5625) is at about z/H = 0.3125 while the neutral level in the cold zone, for the same cross section, is at about z/H = 0.625. This phenomenon may be explained as follows: in the hot zone the velocities near the floor (in x-direction) are higher than those in the upper part of the hot zone (see Figure 5e). The acceleration of the horizontal airflow near the floor as it passes through the aperture from the cold zone into the hot zone is attributed to the three-dimensional characteristics of the airflow and the boundary-layer type of flow. In order to satisfy the continuity equation, the flow area for the reverse velocities in the upper part of the hot zone must be larger. Thus, the neutral velocity level is pushed downward. In the cold zone, the velocities near the ceiling (in x-direction) are higher than those in the lower part of the cold zone. Thus, neutral velocity level in the cold zone is raised. At the height z/H = 0.8125 (Figure 5d) the flow is completely divided by the door soffit. The air in the hot zone has a slow vortex motion while the warm air, after entering the cold zone, flows quickly along the ceiling. There is a region of recirculation in each of the partition corners in the cold zone.

Figure 6 demonstrates the flow patterns, in x-z plane at y/W = 0.5625, for the centrally located opening with five different door heights (i.e., h/H = 1.0, 0.875, 0.75, 0.625, and 0.5). In cases of h/H lower than 0.875, there exists a weak clockwise recirculation region near the ceiling in the hot zone, which was also observed in Nansteel and Greif (1984) and Neymark et al. (1988). This recirculation flow does not make a significant contribution to the convective heat transfer across the door. In this region, since the air velocities near the hot wall are very low, the heat transfer from the hot wall to the adjacent air is mainly by conduction. The active area of the hot wall for convective heat transfer is thus decreased as the door height decreases. This results in a lower Nu number, as shown in Figure 7.

To examine the effects of the location of the moving aperture in y-direction on the Nusselt number, the door size is kept constant for h/H = 0.75 and b/W = 0.25 with the partition located in the middle of the room. The computed results, as shown in Figure 8, indicate that the heat transfer rate increases slightly with the door moving from the center toward the side-wall. It could be understood by examining Figures 9 through 12. Moving the door location from the central position at y_D/W = 0.5 toward the side-wall at y_D/W = 0.875 produces a clockwise vortex flow in the hot zone and another clockwise vortex flow in the cold zone. The vortex flow patterns are different at various elevations, as shown in Figures 9 through 12. For example, consider the case of the door located adjacent to the side-wall y_D/W = 0.875: at the plane of z/H = 0.0625 (Figure 9d), a vortex flow is seen in the hot zone at the front corner of the partition. This vortex moves along the partition toward the opening when the horizontal plane moves up to z/H = 0.3125 (Figure 10d). After the main airflow changes its direction from the hot side toward the cold side, there is a weak vortex appearing in the rear corner of the cold wall (Figure 11d). At the plane z/H = 0.8125 (Figure 12d), where two zones are completely separated by the door soffit, two separate recirculation flows exist in both regions: a large one in the hot zone and a small one in the cold zone. It can be seen that due to the vortex, the velocity component, v,

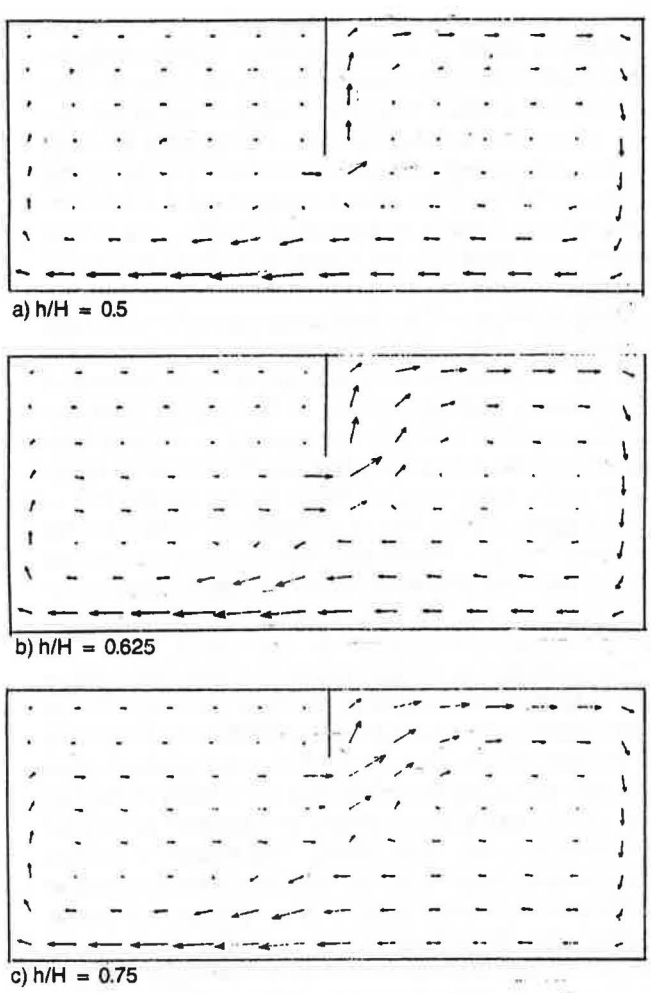

Figure 6 *Flow patterns in x-z planes at y/W = 0.5625 for centrally located opening*

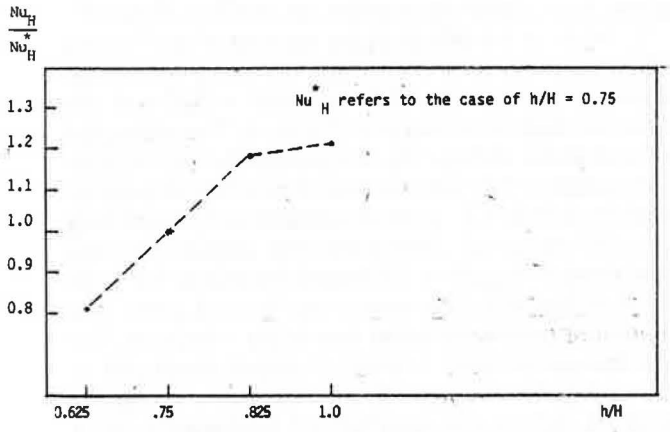

Figure 7 *Nusselt number variation with door height*

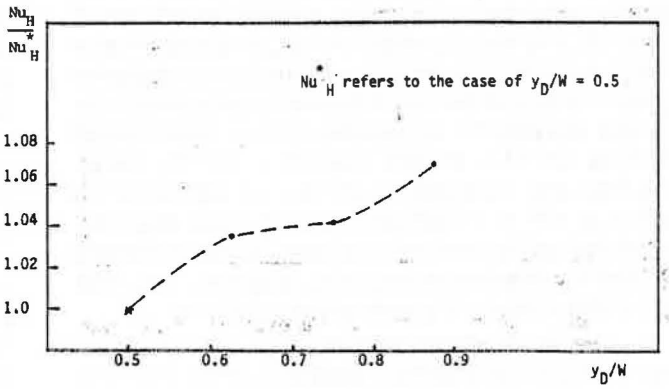

Figure 8 *Nusselt number variation with door location*

increases near both the hot and cold walls, which leads to a favorable convective heat transfer.

To examine the effect of the partition location on the convective heat transfer, the door size (h/H = 0.75 and b/W = 0.25) and its location (x_D/L = 0.5 and y_D/W = 0.5) remain unchanged. Figure 13 shows the air velocity vectors in the x-z planes for three locations of the partition at y_D/L = 0.2857, 0.5, and 0.7143. It can be seen that when the partition moves apart from the central position of the room, there is a redistribution of the two vortex flows in the hot and cold zones. Figures 14 through 17 indicate the air velocity vectors in the x-y planes at z/H = 0.0625, 0.3125, 0.5625, and 0.8125, respectively, for the same three locations of the partition. It should be noted that the change of flow patterns at different partition locations does not significantly affect the convective heat transfer rate. This result is attributed to the very small temperature stratification in the horizontal direction in both the hot and cold zones. The computed

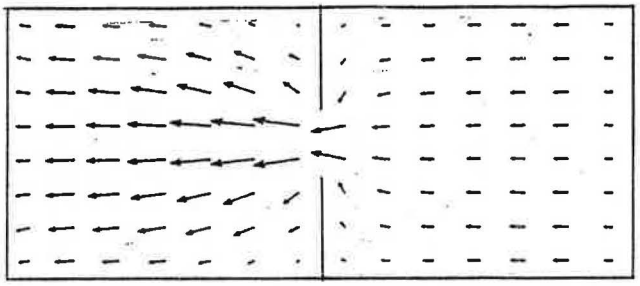

a) yD/W = 0.5

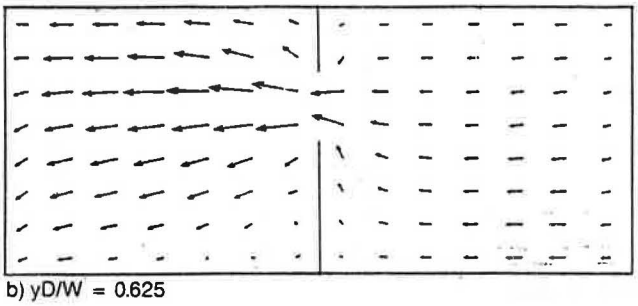

b) yD/W = 0.625

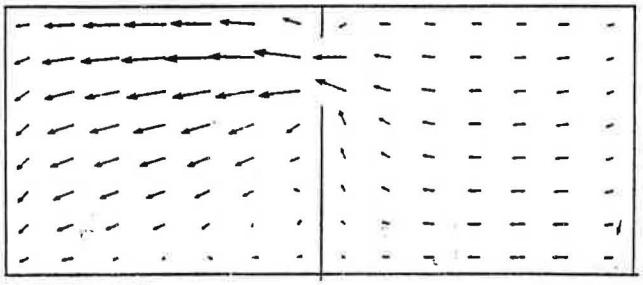

c) yD/W = 0.75

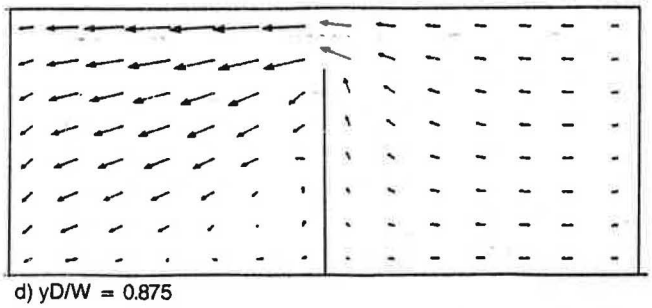

d) yD/W = 0.875

Figure 9 *Variation of flow patterns in x-y planes at z/H = 0.0625 with door location*

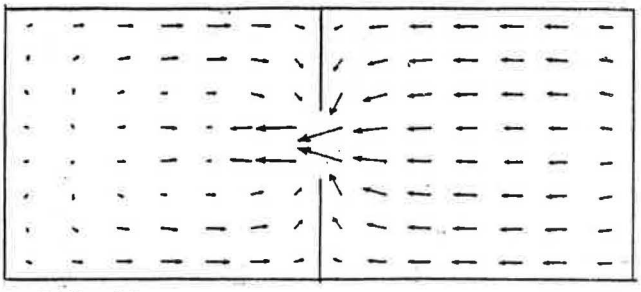

a) yD/W = 0.5

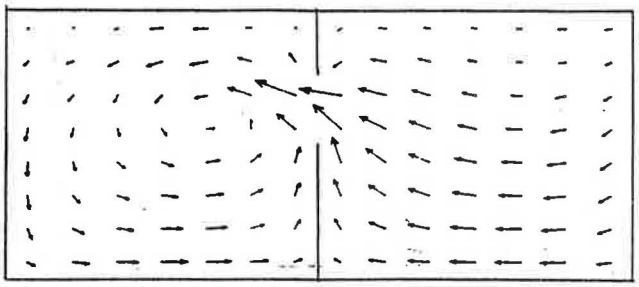

b) yD/W = 0.625

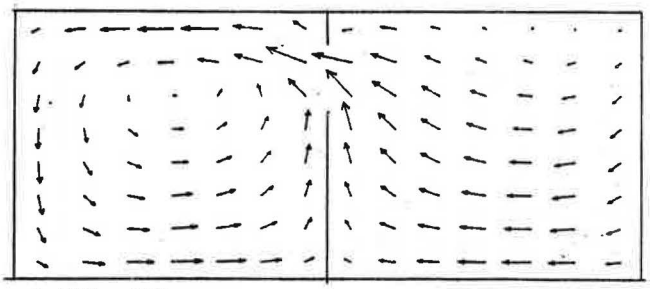

c) yD/W = 0.75

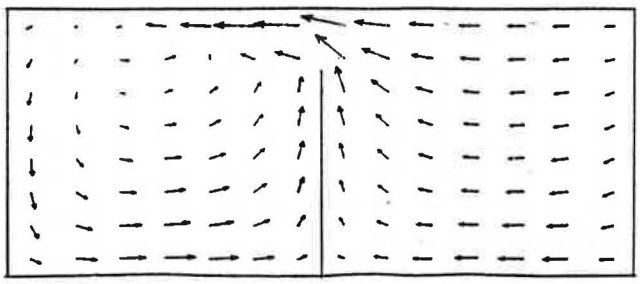

d) yD/W = 0.875

Figure 10 *Variation of flow pattern in x-y plane at z/H = 0.3125 with the door location*

convective heat transfer rates across the doorway represented by the ratio of the Nusselt number, Nu_H, for different locations of the partition to the Nusselt number, $N\mathring{u}_H$, for the central location of the partition as a function of X_D/L are plotted in Figure 18. It shows that the heat transfer rate is not sensitive to the change in location of the partition.

The vertical temperature stratifications in the x-z plane at different horizontal locations for the case of $y_D/W = 0.5$ and $h/H = 0.75$ are plotted in Figure 19. The vertical temperature variation adjacent to the hot wall (curve 1) is larger than that adjacent to the cold wall (curve 4). The temperatures in the upper part near the hot wall are increased rapidly because of the clockwise recirculation in this region, which is separated by the door soffit from the cold zone. The heat in this region is less likely to be transferred through the opening into the cold zone by convection. In the hot zone the temperatures near the partition in the region from $z/H = 0.33$ to $z/H = 0.83$ are even higher than those near the hot wall. This is due to the air coming from the upper part of the opening in the hot zone and from both the side-walls in the y-direction, where the temperatures are

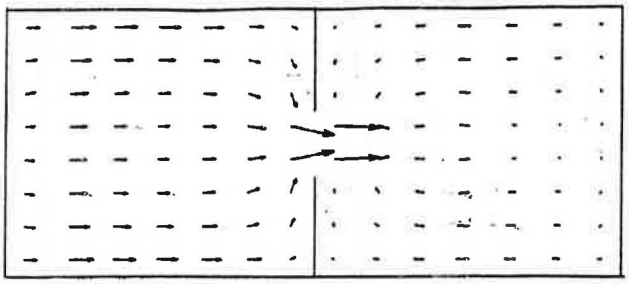

a) yD/W = 0.5

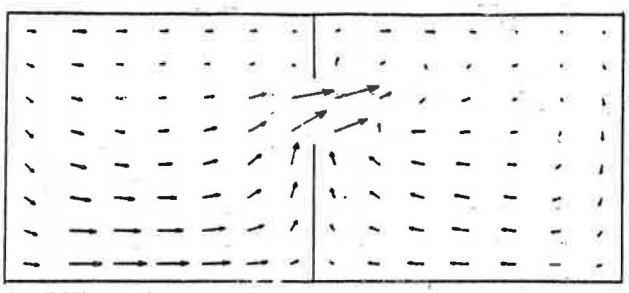

b) yD/W = 0.625

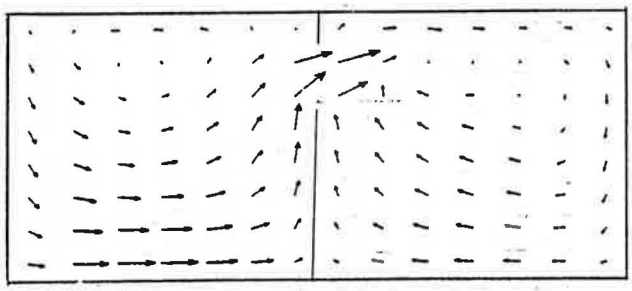

c) yD/W = 0.75

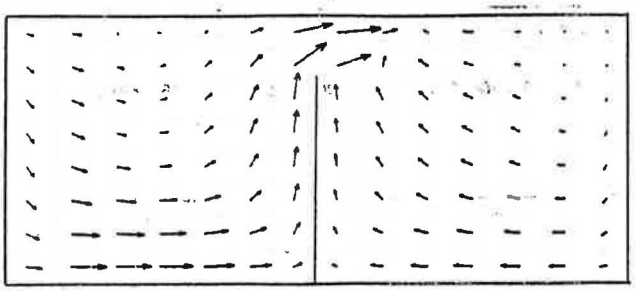

d) yD/W = 0.875

Figure 11 *Variation of flow patterns in x-y plane at z/H = 0.5625 with door location*

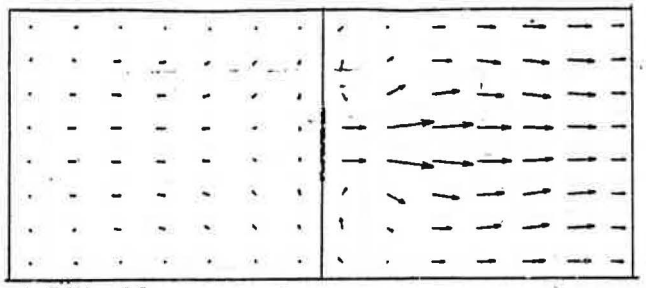

a) yD/W = 0.5

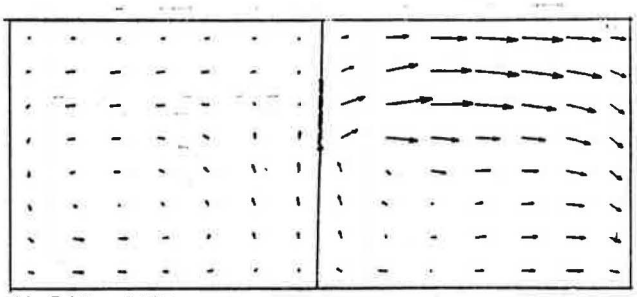

b) yD/W = 0.625

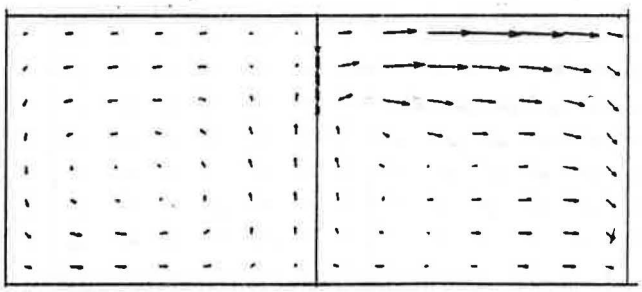

c) yD/W = 0.75

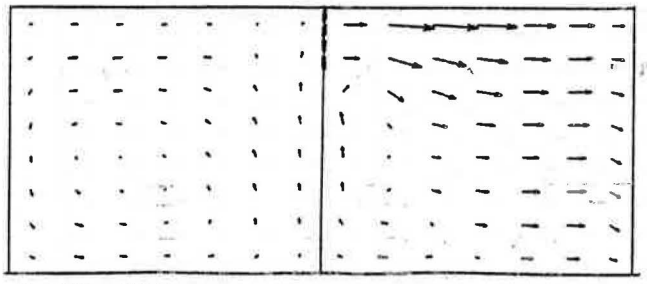

d) yD/W = 0.875

Figure 12 *Variation of flow pattern in x-y plane at z/H = 0.8125 with door location*

higher than the air temperature near the hot wall. In the cold zone, for the same reason, the temperatures near the opening (curve 3) in the range from z/H = 0.12 to z/H = 0.37 are lower than those adjacent to the cold wall (curve 4). These phenomena can only be observed in the three-dimensional airflow model.

CONCLUSIONS

The effect of door size, location, and different partition locations in a room on the pattern of airflow and the convective heat transfer is studied using the k-ϵ two-equation model. The numerical results obtained from this model lead to the following conclusions:

1. The airflow pattern is very sensitive to changes in the door size and location on the partition and to the change in the location of the partition.

2. The heat transfer rate is sensitive to changes in the door height and location on the partition but not sensitive to the change in the location of the partition.

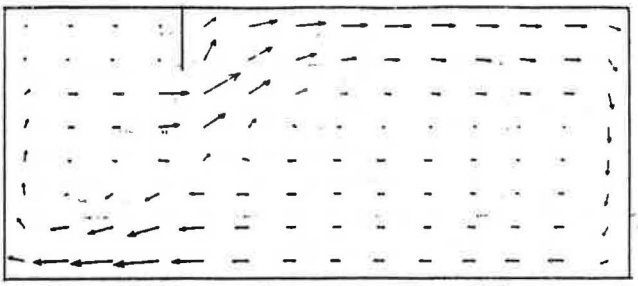

a) xD/L = 0.2857

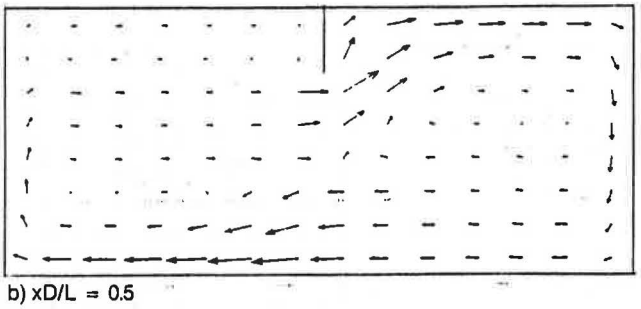

b) xD/L = 0.5

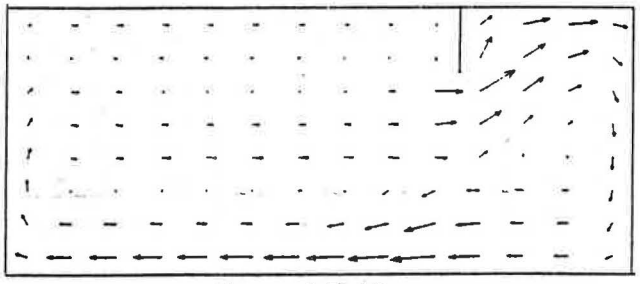

c) xD/L = 0.7143

Figure 13 *Velocity vectors in x-z plane at y/W = 0.5625 for h/H = 0.75*

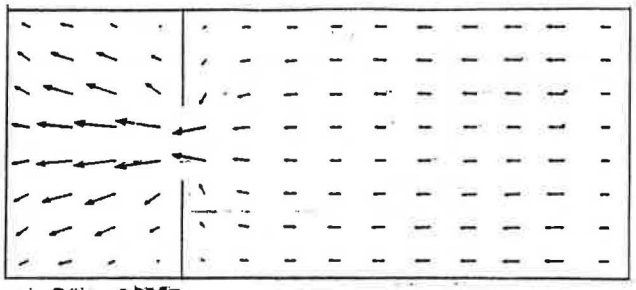

a) xD/L = 0.2857

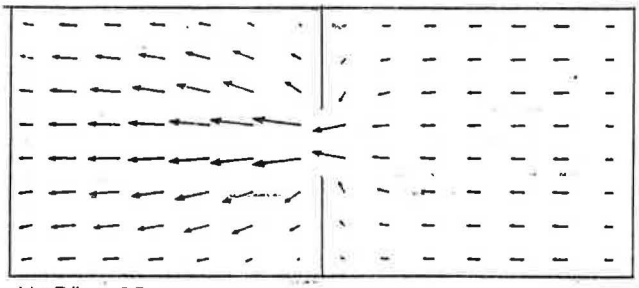

b) xD/L = 0.5

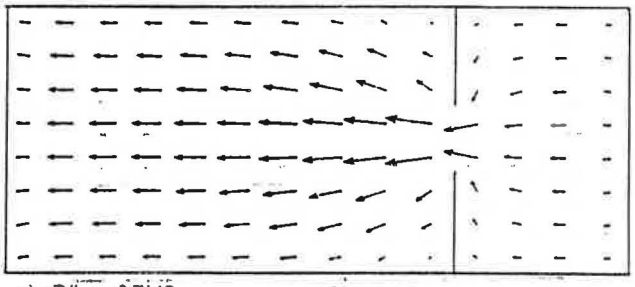

c) xD/L = 0.7143

Figure 14 *Velocity vectors in x-y plane at z/H = 0.0625 for h/H = 0.75*

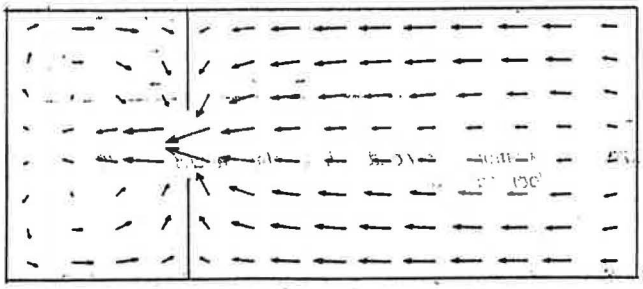

a) xD/L = 0.2857

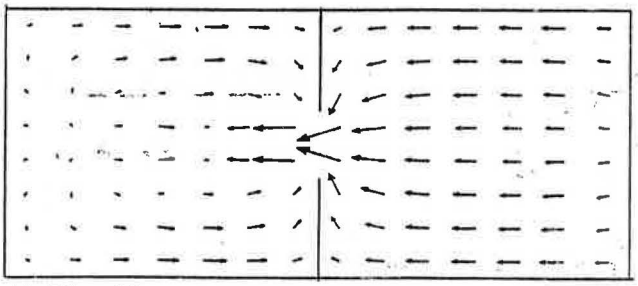

b) xD/L = 0.5

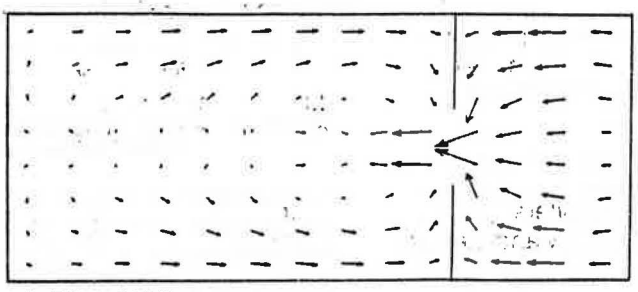

c) xD/L = 0.7143

Figure 15 *Velocity vectors in x-y plane at z/H = 0.3125 for h/H = 0.75*

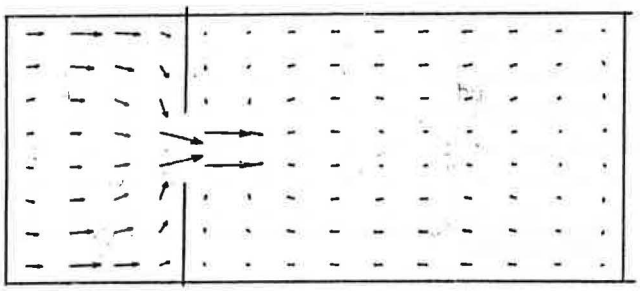

a) xD/L = 0.2857

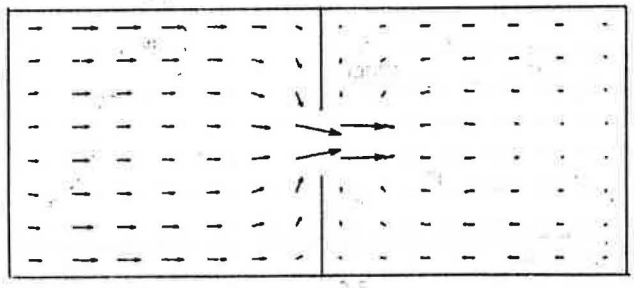

b) xD/L = 0.5

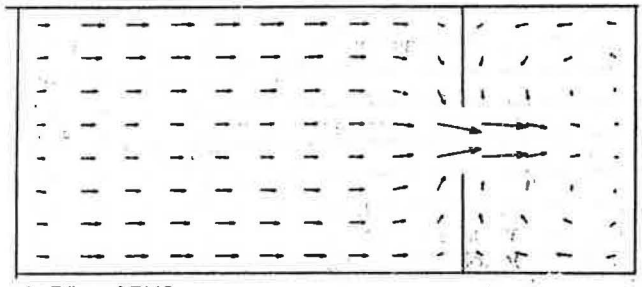

c) xD/L = 0.7143

Figure 16 *Velocity vectors in x-y plane at z/H = 0.5625 for h/H = 0.75*

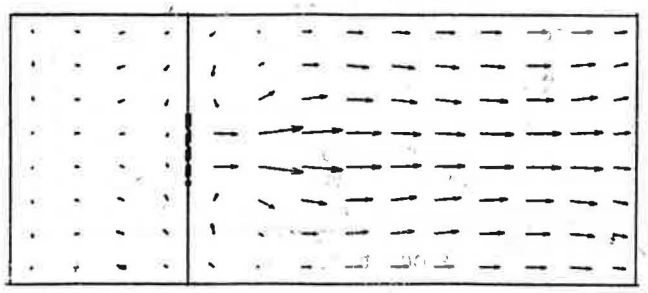

a) xD/L = 0.2857

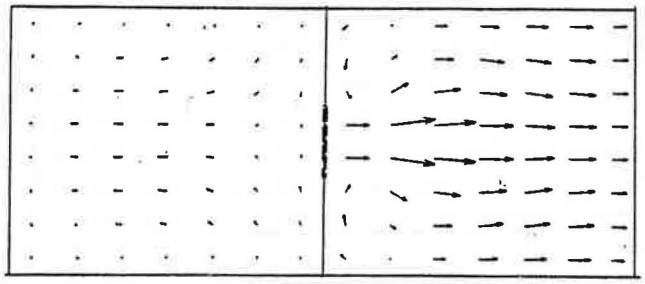

b) xD/L = 0.5

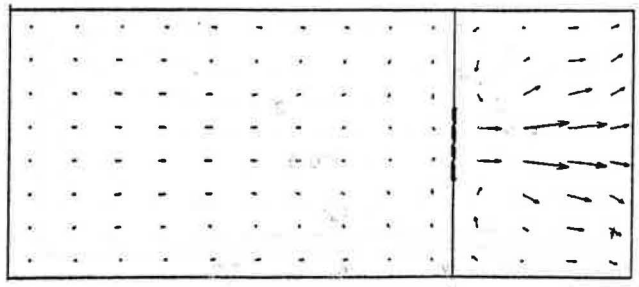

c) xD/L = 0.7143

Figure 17 *Velocity vectors in x-y planes at z/H = 0.8125 for h/H = 0.75*

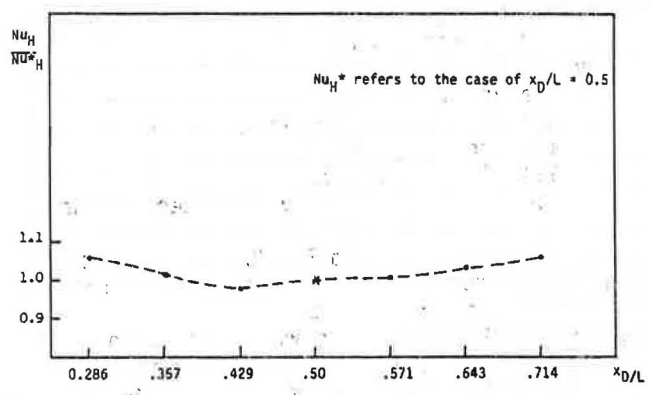

Figure 18 *Nusselt number variation with partition location*

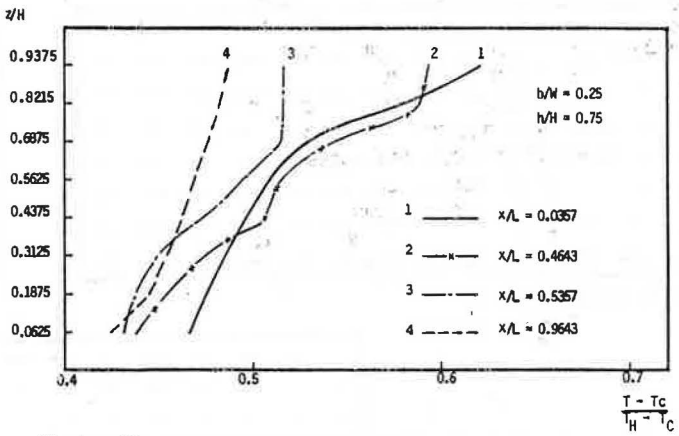

Figure 19 *Vertical temperature stratification in the plane y/W = 0.5625 for the case yD/W = 0.5 and XD/L = 0.5*

3. The neutral level (velocity in x-direction equal to zero) in the hot zone is lower than that in the cold zone.

4. The airflow patterns obtained from the computational model developed provide useful design information for the thermal comfort and contaminant transportation in partitioned enclosures.

5. The agreement between the computed Nusselt number, Nu_L, and that obtained from experimental measurements is very good, which gives confidence for applying this computational model to further studies on interzonal heat and mass transfer.

ACKNOWLEDGMENTS

We wish to express our thanks to the National Research Council of Canada and "Fonds Pour la Formation de Chercheurs

et l'Aide a la Recherche," which funded this study through joint NSERC and FCAR grants.

NOMENCLATURE

b	= door width
D	= diffusion conductance, $\gamma_\phi/\delta x$
F	= convection across unit area at the boundary of control volume, ρu
g	= acceleration due to gravity
G_B	= generation of turbulent kinetic energy, related with buoyancy
G_K	= stress production of turbulent kinetic energy
H	= room height
h	= door height
k	= kinetic energy of turbulence
L	= room length
Nu	= Nusselt number based on room height, $q\,H/(T_H - T_c)\lambda$
Nu_L	= Nusselt number based on room length, $q\,L/(T_H - T_c)\lambda$
Pr	= Prandtl number, ν/α
P	= pressure
Pe	= cell Peclet number, F/D
q	= heat flux
Ra	= Rayleigh number based on room height, $g\beta H^3 (T_H - T_c)/\nu\alpha$
Ra_L	= Rayleigh number based on room length, $g\beta L^3 (T_H - T_c)/\nu\alpha$
R_f	= flux Richardson number, $- G_B/G_k$
S_ϕ	= source term for variable ϕ
T	= temperature
T_o	= reference temperature
T_c	= cold wall temperature
T_H	= hot wall temperature
t	= time
u	= velocity component in x direction
v	= velocity component in y direction
V	= volume of control volume
w	= velocity component in z direction
W	= room width
x,y,z	= coordinate system
X_D	= distance from hot wall to partition
y_D	= distance from y = 0 to the center of the door
$\Delta x, \Delta y, \Delta z$	= dimensions of control volume
α	= thermal diffusivity
β	= coefficient of thermal expansion
γ_ϕ	= exchange coefficient of ϕ
δx	= distance between nodes
ϵ	= dissipation rate of k
λ	= thermal conductivity
μ_{eff}	= effective dynamic viscosity, $\mu_{eff} = \mu_l + \mu_t$
μ_l	= molecular viscosity
μ_t	= turbulent dynamic viscosity
ν_t	= turbulent kinematic viscosity
ρ	= density
σ	= turbulent Schmidt or Prandtl number
ϕ	= variables

Subscripts

p	= currently considered grid
t	= turbulent

REFERENCES

Brown, W.G., and Solvason, K.R. 1962. "Natural convection through rectangular opening in partitions, part 1: vertical partition." *Int. J. Heat and Mass Transfer*, Vol. 5, pp. 859-868.

Chang, L.C.; Lloyd, J.R.; and Yang, K.T. 1982. "A finite difference study of natural convection in complex enclosures." 7th Int. Heat Transfer Conference, Vol. 2.

Cheesewright, R. 1968. "Turbulent natural convection from a vertical plane surface." *Transactions of ASME, Journal of Heat Transfer*, pp. 1-9.

Chen, Q. 1988. "Indoor air flow, air quality and energy consumption of building." Ph.D. Thesis, Delft University of Technology, The Netherlands.

Gadgil, A. 1979. "On convective heat transfer in building energy analysis." Ph.D. Thesis, Department of Physics, University of California, Berkeley.

Gadgil, A.; Bauman, F.; and Kammerud, R. 1982. "Natural convection in passive buildings: experimental, analysis, and results." *Passive Solar Journal*, Vol. 1, No. 1.

Jones, P., and O'Sullivan, P. 1985. "Modelling of air flow patterns in large single volume spaces." SERC Workshop: Developments in Building Simulation Programs, Loughborough University, U.K., October.

Kubleck, K.; Merker, G.P.; and Straub, J. 1980. "Advanced numerical computation of two-dimensional time-dependent free convection in cavity." *Int. J. Heat Mass Transfer*, Vol. 23, pp. 203-217.

Launder, B.E., and Spalding, D.B. 1972. *Mathematical model of turbulence*. London: Academic Press Inc.

Launder, B.E., and Spalding, D.B. 1974. "The numerical computation of turbulent flows." *Comp. Methods Appl. Mech. Eng.*, Vol. 3, p. 269.

Mahajan, B.M. 1986. "Measurement of air velocity components of natural convection interzonal airflow." *Proc. of the Air Movement and Distribution Conference.*

Mahajan, B.M. 1987. "Measurement of interzonal heat and mass transfer by natural convection." *Solar Energy*, Vol. 38, No. 6, pp. 437-446.

Markatos, N.C., and Pericleous, K.A. 1984. "Laminar and turbulent natural convection in an enclosed cavity." *Int. J. Heat Mass Transfer*, Vol. 27, No. 5, pp. 755-772.

Nansteel, N.W., and Greif, R. 1984. "An investigation of natural convection in enclosures with two and three-dimensional partitions." *Int. J. Heat Mass Transfer*, Vol. 27, No. 4, pp. 561-571.

Neilson, P.V.; Restivo, A.; and Whitelaw, J.H. 1979. "Buoyancy-affected flows in ventilated rooms." *Numerical Heat Transfer*, Vol. 2, pp. 115-127.

Neymark, J.; Kirkpatrick, A.; Anderson, R.; and Boardman, C. 1988. "High Rayleigh number natural convection in partially divided air and water filled enclosures." National Heat Transfer Conference, Houston.

Patankar, S.V. 1980. *Numerical heat transfer and fluid flow*. New York: Hemisphere.

Rodi, W. 1984. "Turbulence models and their application in hydraulics—a state of the art review." IAHR, second revised edition.

Scott, D.; Anderson, R.; and Figliola, R. 1988. "Blockage of natural convection boundary layer flow in a multizone enclosure." *Int. J. Heat and Fluid Flow*, Vol. 9, No. 2, June.

Shaw, B.H. 1972. "Heat and mass transfer by natural convection and combined natural and forced air flow through large rectangular openings in vertical partition." *Proc. Int. Mech. Eng. Cong. on Heat Mass Transfer by Combined Forced and Natural Convection*, Manchester, Vol. 819, pp. 31-39.

Weber, D.D., and Kearney, R.J. 1980. "Natural convection heat transfer through an aperture in passive solar heated building." *Proc. 5th Nat. Passive Solar Conference*, Amherst, MA, October 19-26.

Wray, W.O., and Weber, D.D. 1979. "Blast similarity studies; part 1, hot zone/cold zone: a quantitative study of natural heat distribution mechanism in passive solar building." *Proc. 4th Nat. Passive Solar Conference*, Kansas City, Vol. 4, pp. 726-230.